Low-cost, high-precision propagation delay measurement of 12-fibre MPO cables for the CMS DT electronics upgrade

2013 JINST 8 C02001

(http://iopscience.iop.org/1748-0221/8/02/C02001)

PUBLISHED BY IOP PUBLISHING FOR SISSA MEDIALAB

RECEIVED: *October 29, 2012*
ACCEPTED: *December 12, 2012*
PUBLISHED: *February 1, 2013*

TOPICAL WORKSHOP ON ELECTRONICS FOR PARTICLE PHYSICS 2012,
17–21 SEPTEMBER 2012,
OXFORD, U.K.

2013 JINST 8 C02001

Low-cost, high-precision propagation delay measurement of 12-fibre MPO cables for the CMS DT electronics upgrade

Á. Navarro-Tobar,[1,2] **C. Fernández-Bedoya,**[2] **and I. Redondo**[2]

CIEMAT,
Avda. Complutense 40, 28040 Madrid, Spain

E-mail: alvaro.navarro@ciemat.es

ABSTRACT: CMS DT electronics upgrade involves laying down 3500 optical links from the CMS experimental cavern to the service cavern, whose lengths must be matched to minimize skew, so that the present upstream electronics can be reused at an initial stage. In order to assess the cables' compliance, a high resolution and cost-effective system has been developed to measure the length uniformity of these fibres. Transit-time oscillation method has been implemented with matched MTP 12-channel fibre optic transmitter and receiver and a Spartan-6 FPGA. After proper corrections and averaging, millimetre-range accuracy has been achieved.

KEYWORDS: Digital electronic circuits; Manufacturing; Special cables

[1]Corresponding author.
[2]On behalf of the CMS DT group.

doi:10.1088/1748-0221/8/02/C02001

Contents

2013 JINST 8 C02001

1 Introduction

HL-LHC is foreseen to raise the luminosity up to a factor ten, to 10^{35} cm^{-2} s^{-1}, with respect to nominal LHC design. Consequently, some of the electronics in different sub-systems will be upgraded in order to adapt to the increased data rate. For the CMS Drift Tubes (DT) subdetector [1], an upgrade to the second level of the trigger and readout electronics chain, currently placed in the CMS experimental cavern, is in progress [2]. This upgrade will be carried out in two stages, corresponding to the two next long shutdown periods of the accelerator: first, relocation of the current second-level electronics to the CMS service cavern, and second, an upgrade of the electronics to increase performance. The CMS service cavern is a much more accessible area than the CMS experimental cavern. Its environment is free of radiation and strong magnetic field, which provides more ample margin in terms of power supply and dissipation. For this reasons, the necessary upgrade in electronics performance will be most easily and efficiently carried out in this environment, increasing, additionally, the ease of maintenance, and, consequently, reducing the probability of subdetector unavailability.

The twisted-copper pair differential data links currently arriving to the present location of the second-level electronics [3, 4] are being converted in-place to optical fibre in order to cover the

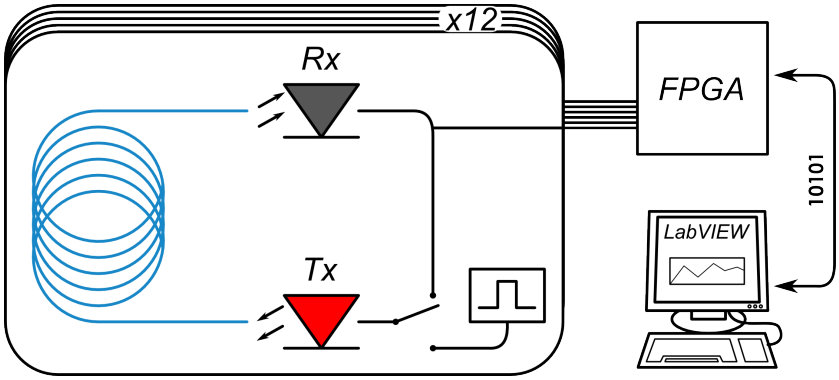

Figure 1. Schematic of the measurement system.

distance to the CMS service cavern. In the second-level electronics of the trigger chain, no per-channel phase adjustment was implemented, and all serial streams arriving to the same board are sampled with the same clock. For this reason there are strict requirements on channel-to-channel skew, and thus the fibres' propagation delays have to be characterized. The maximum acceptable delay difference between two of these fibres has been established in 1 ns. The fibres are arranged in 60 trunk cables, 96 fibres each, for a total of 480 MPO fibre cords [2].

In view of this high number of links, a simple and fast system is needed. Common systems available in the market, based in time-domain reflectrometry [5], are expensive and/or low resolution (∼20 cm), and usually oriented to single fibre measurement and not 12-channels MPO cord, increasing significantly the required time of the operation. A parallel-optics, simple and fast system has been built to measure fibre length with high precision, and is presented in this work.

2 System description

Since fibre validation is to be done before the installation, both ends of the cable are available for the test, and transmission methods can be used instead of the more-demanding reflectometry ones. The transit-time oscillation method [6] has been implemented for this purpose. It consists in driving the optical fibre with a short-duration pulse and feeding signal from the receiver in the other end back to the transmitter, creating a self-sustained oscillation. The fibre propagation delay is one of the terms contributing to the period of this oscillation, and can be calculated from its frequency once the other terms are characterized. This method allows obtaining an accurate measurement of the transit time by averaging multiple periods, instead of using a complex time-to-digital converter to measure one (or several) single edges accurately. It is worth noting that the advantages implied by the measurement of the oscillation period instead of the timestamp of an edge are not exclusive of transit-time measurement systems, as a pulse-reflection-oscillation method, that requires access to only one of the ends, can also be implemented [7]. However, in our case, the availability of both fibre ends favours the election of the former method for its simplicity.

The transmitter and receiver are 12-channel MTP modules from Avago Technologies (HFBR-772 & HFBR-782) [8] that support data rates up to 2.7 Gbd. The oscillation-starting pulse is injected into the loop by a 1-to-16 LVDS clock distribution chip which is disabled for the oscillation

2013 JINST 8 C02001

measurement. The parallel differential feedback bus is AC-coupled, what causes the duty cycle to stabilize at 50% after a few cycles. This bus is read and the frequency measured separately in each one of the 12 channels by the Spartan-6 FPGA present in a SP605 evaluation board. This FPGA also drives the clock distribution chip for initial pulse injection, and communicates with a computer through a serial link for process control and measurement readout. The computer runs a LabVIEW program that allows automatic cable testing. The electronic system (transmitter, receiver, FPGA, cooling and power supply) was packed in an aluminum box. A schematic of the system is shown in figure 1.

3 System calibration

Fibre homogeneity can be expressed both in terms of length and delay. As is well known, the conversion factor between these two magnitudes is given by the speed of light and the fibre optic refractive index, which is a vendor-provided parameter. For the fibres under test, the refractive index specified in the datasheet is 1.482. However, other factors can alter this relationship, e.g. the cord's bending radius or the operating temperature. Since the system used provides a measurement of the propagation delay, calibration and accuracy determination have been done in units of time. In this section, we discuss the calibration of the system for the accurate measurement of the propagation delay of a fibre optic cable, which is considered constant and stable. It doesn't account for variations in this propagation delay caused by the modification of ambient temperature or the manipulation of the cord.

Since the fibre's contribution to the total oscillation period is considered constant, the accuracy of the measurement will be limited by the stability of the system's contribution to the oscillation period and the accuracy with which it can be determined.

3.1 Resolution

In each measurement cycle, the FPGA uses its internal clock to measure the time elapsed until a user-specified number of edges is detected in the electrical feedback part of the loop. The averaged, 3-byte period reading is output through the serial link to the computer, so that resolution is 0.15 ps, and the measurement range is 0–2.56 μs. The integration time is, thus, selectable; in our case it was set to approximately 325 ms, which corresponds to counting 2^{20} edges of the 310-ns period oscillation induced in the 62-m fibre link being tested.

The measurement range is enough for our goals, as well as the resolution, since it is finer than other errors present in the measurement. However, the FPGA can be easily re-programmed to suit other measurement needs.

3.2 Temperature

Variations in temperature produce changes in intrinsic characteristic of semiconductors, such as drift and diffusion coefficients or intrinsic carrier density, and this, in term, affects the temporal behaviour of all electronic and electro-optical components (amplifiers, lasers, pin photodiodes) [9] in both transmitter and receiver. The datasheet of these modules states that "an EEPROM and state machine are programmed to provide both ac and dc current drive to the laser to ensure correct modulation, eye diagram and extinction ratio over variations of temperature and power supply

2013 JINST 8 C02001

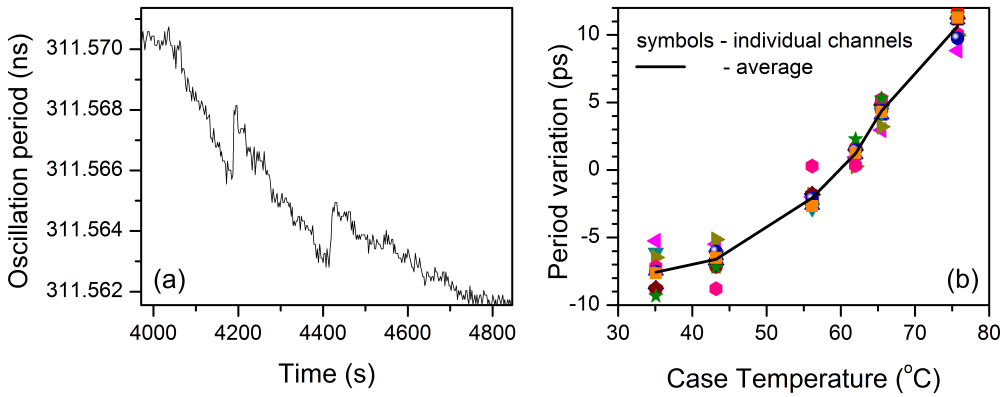

Figure 2. (a) Evolution of the oscillation period with time while cooling is taking place. (b) Variation of period vs. case temperature.

voltages" [8]. In order to assess the influence of temperature in the system's contribution and the effectiveness of the correcting mechanism, the system was operated with a 62-m fibre cord and the oscillation period measured under different environmental conditions, varying the temperature and flow of an air blower directed towards the heat sinks of the receiver and transmitter modules.

Several steps in the (2–2.5) ps interval were observed (for example, in the register plotted in figure 2a), especially linked with periods of variation in the devices' temperature. These are attributed to the corrections in current drive carried out by the transmitter and receiver modules.

The oscillation period was registered for all 12 channels, together with 6 measurements of the temperature of the transmitter's and receiver's heat sink, obtained with a 80T-IR Fluke infrared temperature probe. In order to be able to position the temperature probe, this measurement was done with the aluminum box open. Figure 2b shows the scatter plot of the variation of period of the different channels and their average against the average value of both modules' heat sink temperature, which was varied from 35 ^{o}C to 75 ^{o}C. The lowest end of the temperature range was obtained by blowing room temperature air into the heat sinks, and higher temperatures were produced by blowing air from a 1 kW heater straight into the modules. The actual measurement conditions with the aluminum box closed and a room temperature of $\sim$25 ^{o}C correspond to a heatsink temperature of approximately 65 ^{o}C, as calculated by comparing the periods measured on the same cord under both conditions. As it can be seen, the dependence of period on temperature is small at low temperature, of approximately 0.1 ps/K, increasing to up to 0.7 ps/K at the higher temperature range (which corresponds with the actual closed-box measurement conditions) for a full range variation of 20 ps.

If temperatures are kept stable and at comfort levels, the error produced by temperature variations should remain in the range of 5 ps. Additionally, since a change in the state machine can occur at any moment with any small variation of temperature, the measurement is also subject to a 2.5 ps inaccuracy.

3.3 Transient response

The transient before reaching an stable operating regime can take some time after a long period of unpowered storage, or even after the disconnection and reconnection of the fibre cord. In order to

2013 JINST 8 C02001

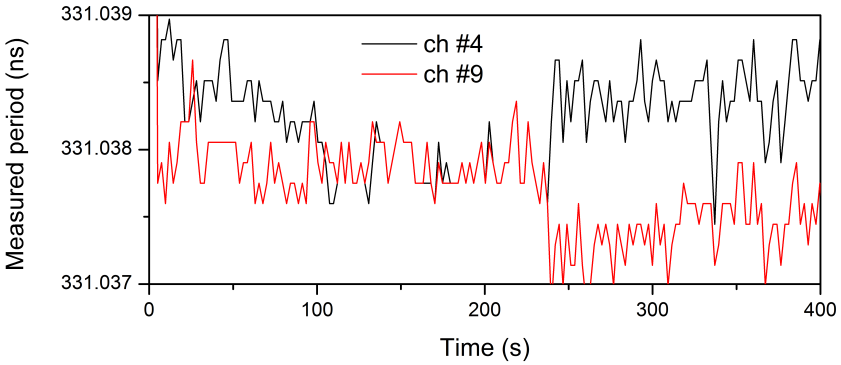

Figure 3. Measured period over time for two closely-matched channels.

assess this stabilization time and to be able to measure correctly, as well to evaluate medium-term stability of the system, the evolution of the oscillation period was monitored with a 62 m cord connected, after several hours disconnected from the power supply, and after fibre cord disconnection of 30 s and 300 s.

In the first case, variations observed after 1000 s of operation were smaller than 1 ps. 60 s after startup the measurement was deviated 6 ps from the final value, and after 300 s it was only 3 ps away. No noticeable variation was observed in the measured oscillation period after disconnecting the fibre cord for 30 s or 300 s.

A large, isolated step with 20 ps of amplitude was, however, observed in one of the channels, not associated with any recognizable change in the state or environment of the system. Although this step was unique and not possible to reproduce, the chance of it happening again is unforeseeable and should be taken into account when evaluating the final system's accuracy and reliability.

3.4 Number of active channels

The number of active channels has the potential to affect the measurement due to the different thermal dissipation that the transmitter and receiver have depending on the kind of signal. In order to test this, the 12 channels were disconnected sequentially. After approximately half of the channels are disconnected, strong steps associated with each new disconnection are observed in the remaining channels. These steps are in the (0–150) ps range.

These strong variations have not been considered for the evaluation of the system's accuracy, because the disconnection of individual channels is not part of the intended use procedure, and, in fact, the lack of transmission in any subset of the channels would indicate a defective cable.

3.5 Cross talk coupling

Channels with similar propagation delays (within 15 ps of each other) were found to couple due to edge synchronization. This phenomenon can be observed in figure 3, in which the coupling and de-coupling of two channels over time is shown. The cross talk coupling distorts the period measurement and can happen at any time with similarly lengthed fibres, although, luckily, it is easily recognizable since the two channels show extremely well matched delays.

This coupling is probably due to a high extent to the fact that, because of the tight packing of the optical modules' footprint pads, the pcb tracks corresponding to different pairs run closely

2013 JINST 8 C02001

spaced and parallel for several millimetres. However, this phenomenon was also observed, although with smaller difference in their respective intrinsic oscillation period, between channels whose electrical paths are completely apart. Since we can safely assume that cross coupling along the optical path is negligible, some coupling must exist within the optical modules. The datasheet [8] acknowledges this possibility and integrates its effect into the maximum contribution to the total jitter specification, which is 160 ps.

3.6 Calibration at operating conditions

The system's contribution to the loop delay has to be characterized as a function of the oscillation period in order to properly use the system to measure the absolute fibre optic propagation delay or length. Note that for the measurement of fibre differences, expected to be in the nanosecond range, this calibration is not strictly necessary. This contribution (τ) can be written as a Taylor series as a function of either the total oscillation period (T) or the fibre propagation delay (t):

$$\tau = \sum_{i=0}^{\infty} a_i \cdot T^i = \sum_{i=0}^{\infty} b_i \cdot t^i$$

$$T = t + \tau$$

The characterization of τ has been done in three stages. First, it was verified that the contributions due to Taylor terms higher than one (corresponding to the function's curvature) could be disregarded. Next, the magnitude of the first-order term was evaluated. Finally, the zeroth-order term (offset) was determined.

3.6.1 Curvature

The oscillation period was characterized with different combinations of three fibre cords (A, B and C): A, A+B, A+C, A+B+C. The fibre propagation delay, as well as the zeroth- and first-order terms of the system's contribution (expressed as a Taylor series of the fibre propagation delay t) cancel, leaving only the second and higher order terms, by making the following algebraic combination of the measured oscillation periods:

$$T_{\mathrm{A}} + T_{\mathrm{ABC}} - \left(T_{\mathrm{AB}} + T_{\mathrm{AC}}\right) = \sum_{i=2}^{\infty} b_i \cdot t^i$$

Two measurements were done, one with A cord of 62 m length, B and C of 2 m (310 ns and 10 ns, respectively) and another with three 62-m cords. The higher-than-one terms contribution was evaluated for all 12 channels, resulting in values 0.4 ps $\pm$ 2 ps (first case) and 2.3 ps $\pm$8 ps (second case). Thus, we conclude that we can safely neglect the contribution from these terms without incurring in a noticeable error. Although we have concluded that we can safely assume that $i \geqslant 2 \Rightarrow b_i \approx 0$, it can be proven that this also holds true for the a_i coefficients.

3.6.2 First order

The first order term can be evaluated by connecting a 62 m fibre cord and taking, in addition to the standard period measurement (T_1), a measurement in which a double oscillation is injected in the loop (two light pulses per period, apparent period $T_2 \approx T_1/2$). Under these conditions, and nulling

2013 JINST 8 C02001

the higher-than-one terms, the fibre propagation delay and the zeroth order term cancel, but the first order term remains:

$$T_1 - 2T_2 = a_1 \cdot (T_1 - T_2)$$

A 62 m cord was used for this measurement, and the first order term was calculated for all 12 channels, averaging to a value of $a_1 = (-49 \pm 4) \cdot 10^{-6}$ (dimensionless). Although a higher operating frequency is expected to cause an increase in delay because of the higher power dissipation and temperature, a power increase of 30 % would be necessary to explain the delay variation when switching from 3.2 MHz to 6.4 MHz, and it can be verified that this is not the case. A feasible explanation to the magnitude of the a_1 coefficient is based on the fact that the receiver is internally AC-coupled (100 kHz cutoff frequency) and that the feedback bus is also AC-coupled with a similar time constant. The period of the signals being considered is not so short so as to disregard the effect of the high-pass filter: right before each edge, the differential signal has diminished due to de effect of filtering, and this contributes to a faster switching of the following stage during the transition. The shortening of the rise/fall time is more pronounced the longer the oscillation period is, and can be expected to produce an effect of the same order of magnitude as the measured a_1 value.

The linearity of this effect should hold well whenever the oscillation period is still much lower than the filters' time constant (10 μs), which fits with the typical use scenario of these kind of multimode fibre links.

In the case of the fibre links we are characterizing, this effect accounts for approximately 15 ps of the total oscillation period. If the measured propagation delay is used to calculate the cord's length, the correction of this effect ($\sim$ 3 mm) would be an order of magnitude smaller than the caused by the limited precision with which the refractive index is known, which is also a first order effect.

When comparing the propagation delay of two fibre links like the ones we are using, the error committed due to the effect of neglecting the nonzero first-order term in the system's contribution to the period is less than 0.1 ps, far below many other sources of error previously characterized.

3.6.3 Offset

The zeroth-order term, the offset, can be characterized [6] by measuring the oscillation period of two different cords (A, B) and the oscillation period with both of them connected (A+B). In order to do so, and since both A and B cords have to be female-female to be able to connect to the optical modules, a means to properly align the fibres had to be provided. Two 0.69 mm diameter rods were cut and introduced in the holes of one of the female MTP connectors to convert it to male. The first-order term cancels in the equation and higher-order terms have already been ruled out, so we have:

$$T_{\mathrm{A}} + T_{\mathrm{B}} - T_{\mathrm{AB}} = a_0$$

The offset was calculated for multiple combinations of the 8 cords available in one trunk cable, and values between 2.25 ns and 2.5 ns were obtained for each of the 12 channels. The calibration values have been plotted in figure 4.

2013 JINST 8 C02001

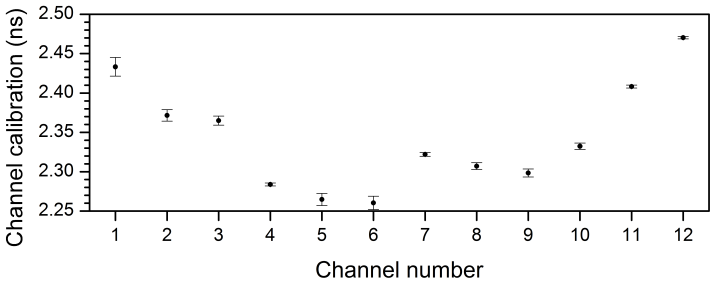

Figure 4. System's zero-order contribution to the measured oscillation period.

3.7 Measurement limits

There is a physical limit to the maximum oscillating frequency ($\sim$ 400 ps) and the minimum period the FPGA is able to measure in its current configuration ($\sim$60 ns). However, smaller propagation delays can easily be measured by adding a known optical offset (a male-female fibre cord) to the measurement.

On the other side, since the fibre optic modules are AC-coupled, slow oscillations ($>$ 20 us, see 3.7.2) cannot be sustained, which bounds the measurable frequency range from below. However, if the overall length of the cable is known, a measurement can be obtained by injecting a higher number of pulses in the loop.

3.8 Accuracy

Considering all the error sources exposed and imposing reasonable conditions to our measurement procedure, we have calculated the accuracy of our system for the measurement of fibre propagation delay differences to be 30 ps, which is good enough for our delay-matching needs.

4 Cable assessment

The present trigger electronics are capable of correctly receiving and deserializing the data stream with variations in the delay of up to $\pm$6 ns. In order to have a reasonable margin of security, the manufacturer was demanded to comply with the following homogeneity specification: at least 4 cords in each trunk cable must have all of its fibres within a 1 ns interval. All the cords in one of the trunk cables were measured and offset-corrected. In figure 5a, the histogram for the difference between each fibre's propagation delay and the corresponding cord's average propagation delay has been plotted. In figure 5b, the histogram for the absolute propagation delay of all fibres has been plotted. In the subsequent discussion, a distance value in cm is given in parenthesis, in addition to the time value in ns, for easier visualization of the magnitudes involved. However, this value is dependent on the actual index of refraction, which is not known with precision, and possibly varies from fibre to fibre.

For each MTP cord, the delays were found to be closely matched, with $\sigma = 0.13$ ns (2.7 cm), being 0.65 ns (13 cm) the maximum difference observed. For the trunk cable, delays are matched with $\sigma = 0.4$ ns (8.2 cm), maximum difference $= 1.5$ ns (30 cm). Two 4-cord subsets can be chosen with maximum difference $<$ 1 ns: 0.55 ns and 0.89 ns (11 cm and 18 cm). These results are in compliance with the stated homogeneity requirement.

2013 JINST 8 C02001

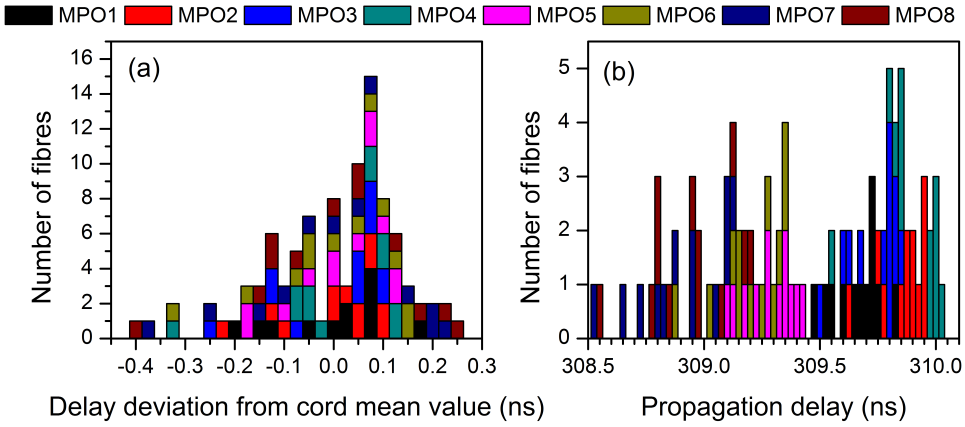

Figure 5. (a) Histogram for the propagation delay difference to the mean value of the corresponding MTP cord. (b) Histogram for the absolute propagation delay of all measured fibres.

Since fibre bending can affect delay, tests were done to assess the possible impact of different routing in the detector. Several qualitative bending tests were carried out: 5-cm radius bending of an individual cord, 20-cm of the trunk, deformation of the whole 50-cm rolled trunk by 10 cm, application of torsion and transversal compressive force to the trunk cable. The strongest delay modification was observed when deforming the whole rolled trunk, and was found to be negligible ($<$ 25 ps).

5 Conclusion

The transit-time oscillation method is easy and relatively inexpensive to implement, and yields excellent results in terms of accuracy for propagation delay measurements. We have built a system based on this method for the simultaneous measurement of the propagation delay of the 12 fibres in a MTP cord, and we have characterized it. With the appropriate measurement aids, the measurement range limits are virtually inexistent. The sources of random error have been studied, and the deterministic error calibrated, resulting in an accuracy of 30 ps.

The system has been used to characterize the propagation delay differences existing in an 8-cord trunk cable. The differences comply with the requirements required to the manufacturer.

References

[1] CMS collaboration, *The CMS experiment at the CERN LHC*, 2008 *JINST* **3** S08004.

[2] C. Fernández-Bedoya, *Muon DT upgrade*, CMS-CR-2011-305 (2011).

[3] L. Guiducci, *DT sector collector electronics design and construction*, in the proceedings of the *Topical Workshop on Electronics for Particle Physics (TWEPP2007)*, September 3–7, Prague, Czech Republic (2007).

[4] C. Fernández-Bedoya, *CMS DT chambers read-out electronics*, in the proceedings of the *Topical Workshop on Electronics for Particle Physics (TWEPP2007)*, September 3–7, Prague, Czech Republic (2007).

2013 JINST 8 C02001

[5] R.H. Cole, *Time domain reflectometry*, *Annu. Rev. Phys. Chem.* **28** (1977) 283.

[6] M. Johnson and R. Ulrich, *Fibre-optical strain gauge*, *Electron. Lett.* **14** (1978) 432.

[7] W.C. Liu and M.H. Lu, *The measurement of propagation delay in multimode optical fibre with pulse-reflection-oscillation method*, *Opt. Laser Technol.* **36** (2004) 81.

[8] *HFBR-778 and HFBR-782 pluggable parallel fiber optic modules, transmitter and receiver*, Data Sheet, Avago Technologies (2008).

[9] S.M. Sze and K.K. Ng, *Physics of semiconductor devices*, John Willey and Sons Inc., Hoboken U.S.A. (2006).

2013 JINST 8 C02001